

Some Measurements of Acoustic Normal Mode Propagation in Shallow Water

A. F. SCHUETZ

*Shallow Water Surveillance Branch
Acoustics Division*

November 16, 1972



NAVAL RESEARCH LABORATORY
Washington, D.C.

CONTENTS

Abstract	ii
Problem Status	ii
Authorization	ii
INTRODUCTION	1
ANALYTICAL MODEL	2
Theoretical Formulation	2
Influence of Sound Speed Profile on Modal Propagation Characteristics	3
EXPERIMENTAL PROCEDURES	8
PROCESSING TECHNIQUES	10
Mode Resolution by Time of Arrival	10
Mode Resolution by Spatial Filtering	10
Measurement of Pressure Amplitude Distribution	11
Measurement of Mode Attenuation Coefficients	11
RESULTS	12
Comparison of Measured and Calculated Vertical Distribution of Pressure Amplitude	12
Mode Attenuation Coefficients	12
Temporal Variations	15
CONCLUSIONS	17
ACKNOWLEDGMENTS	18
REFERENCES	18

ABSTRACT

Experiments were conducted in the northern Gulf of Mexico ($30^{\circ}00'06''$ N, $85^{\circ}54'03''$ W) during July 1969 and March 1970 to study propagation characteristics of acoustic normal modes. This shallow-water area had a constant depth (31 ± 2.5 m) over a propagation path of at least 20 km along a bearing line of 285° T. Short-pulse, 3 cycle signals were emitted from 400- or 750-Hz center frequency sources. The vertical distributions of pressure amplitude of each of the two lowest order normal modes of these signals, measured by a vertical line of hydrophones, agreed well with distributions calculated by computer using a two-layer fluid model. Temporal variations of modal intensity averaged over depth for both the first and the second modes were observed for 7-min runs. Although the specific causes of these variations were not determined, there were indications that the vertical distributions of pressure amplitude remained comparatively stable and signal fluctuations were occurring uniformly with depth. Time-averaged attenuation coefficients were also obtained for the first and second modes for 7-min runs. When a mode was predicted to interact strongly with the bottom, its measured attenuation was high compared to cases where that mode was predicted to interact weakly with the bottom.

PROBLEM STATUS

This is an interim report; work is continuing on the Problem.

AUTHORIZATION

NRL Problem S01-45
Projects RF 05-552-404-5350 and SF 52552-070

Manuscript submitted August 30, 1972.

SOME MEASUREMENTS OF ACOUSTIC NORMAL MODE PROPAGATION IN SHALLOW WATER

INTRODUCTION

Validation tests of normal mode acoustic propagation theory have been conducted in a shallow-water area of the Gulf of Mexico. Acoustic sources were mounted on a fixed platform, a facility of the Naval Ship Research and Development Center, located approximately 20 km offshore from Panama City, Florida, in a water depth of 31 m. The acoustic field was sampled by a vertical line of hydrophones suspended from the USNS GIBBS (T-AGOR-1).

The objective was to compare the vertical distribution of pressure amplitude in individual normal modes of propagation with those predicted by an idealized wave theory model (1) of the area. The field of short, gated sine wave pulses was sampled from near the surface to near the bottom at several ranges along a fixed bearing line. Since the group velocities of signals propagating in discrete normal modes are in general different from mode to mode, the modal arrivals in some cases could be separated by time of arrival. In those cases where individual modes were resolvable, the vertical distributions of pressure amplitude were measured and compared with the theory. In addition, measurement of the modal field intensities permitted the calculation of mode attenuation coefficients.

Two experiments were conducted over the same propagation path; one was in July 1969 and the other in March 1970. In the first experiment a frequency of 400 Hz was used and the vertical line of hydrophones contained eight uniformly spaced elements. The prevailing sound speed profile had a negative gradient. During the second experiment a frequency of 750 Hz was used and the number of elements in the line of hydrophones was increased to twelve. The variety of observed sound speed profiles included positive, zero, and negative gradients.

A previous report (2) described the analytical model and the experimental technique used in these experiments and presented the mode attenuation data obtained during the first experimental period. The present report documents the results obtained from the second set of experiments together with some additional analysis of the July 1969 data. Included are calculations of attenuation coefficients for the first and second modes at 750 Hz and for the first mode at 400 Hz, and a comparison of measured and calculated pressure amplitude distributions for these two modes at both 400 and 750 Hz. A spatial filtering technique, based on the orthogonal property of normal modes, is described. The output of such a filter is used to calculate the modal attenuation coefficients and to examine the temporal stability of the modal intensities averaged over depth.

ANALYTICAL MODEL

Theoretical Formulation

The model used to predict the modal vertical pressure amplitude distribution and group velocities assumes the following environmental constraints: (a) the water layer depth H is constant along the propagation path; (b) the water layer has a constant density ρ_1 and a sound speed $c_1(z)$ which is only a function of the depth z ; and (c) the bottom is a semi-infinite fluid of constant density ρ_2 and constant sound speed c_2 . The geometry of this model is shown in Fig. 1.

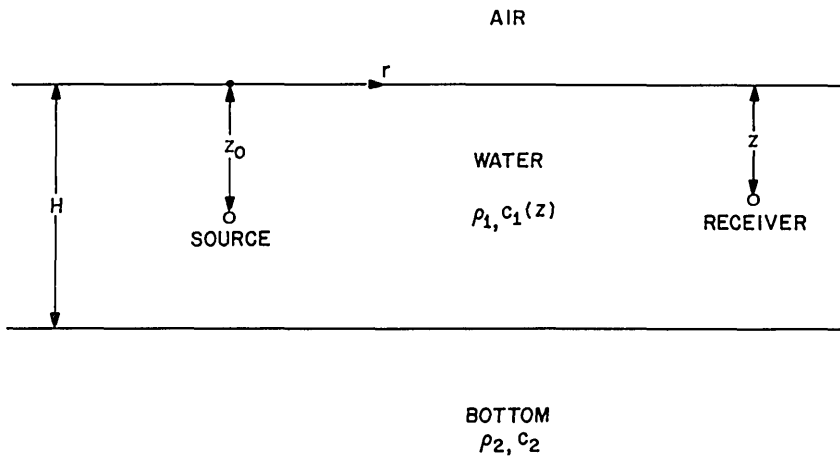


Fig. 1 — Geometry of two-layer analytical model

The pressure amplitude P_n of the n th mode established by a pulsed signal emitted from an omnidirectional point source of center angular frequency ω and unit source strength positioned at a depth z_0 can be related to the free-field source level S , expressed in decibels relative to 1 dyne/cm² at 1 m by (2),

$$20 \log P_n(r, \zeta) = S + 20 \log \left[\frac{\sqrt{2\pi} \rho_1 u_n(\zeta_0) u_n(\zeta)}{H k_n^{1/2}} \right] - 10 \log r \quad (1)$$

$$+ 10 \log \left(\frac{T_0}{T_0 + \Delta T_n} \right) - \alpha_n r.$$

Here

n is the mode number

r is the range from the source

$\zeta = z/H$ is the normalized depth

k_n is the horizontal component of the wave number for the n th mode

T_0 is the pulse length at the source

ΔT_n is the change in pulse length for the n th mode at range r (due to dispersion)

α_n is the attenuation coefficient of the n th mode.

$u_n(\xi_0)$ and $u_n(\xi)$ are the eigenfunctions of the n th mode evaluated at the depth of the source and the depth of the receiver, respectively.

The first two terms on the right side of Eq. (1) represent the equivalent source level for the n th mode. The second term, the mode excitation function, expresses the decrease in the n th mode signal level from the free-field level S . A typical value of this decrease for these experiments is -20 dB. The third term, $10 \log r$, represents cylindrical spreading. The fourth term, $10 \log T_0/(T_0 + \Delta T_n)$, is an approximation of the decrease in peak pressure amplitude in a short pulse caused by the dispersive lengthening of the pulse. The last term, $\alpha_n r$, represents the modal attenuation at range r . Attenuation results from a number of mechanisms such as absorption in the water, scattering by the boundaries and by inhomogeneities in the water, generation of shear waves in the bottom, and absorption in the material of the bottom. In the present stage of development of the analytic model, only the summed effect of all loss mechanisms associated with interaction with the bottom is treated.

Of the factors occurring in Eq. (1), k_n and $u_n(\xi)$ were calculated by a normal mode computer program using an iterative finite difference technique (3). The input parameters of this program were the water and bottom densities, ρ_1 and ρ_2 , respectively; the water sound speed profile $c_1(z)$; the bottom sound speed c_2 ; the water depth H ; and the source center angular frequency ω . This program also calculated the mode group velocities U_n , given by

$$U_n = \frac{\partial \omega}{\partial k_n}. \quad (2)$$

Influence of Sound Speed Profile on Modal Propagation Characteristics

A variety of vertical sound speed profiles was observed during the March 1970 experiment. Profiles a, c, and j (see Tables 1 and 2) are measured examples of negative, zero, and positive gradient profiles, respectively. Their influence on modal propagation characteristics maybe examined for a fixed source center frequency (in this case, 750 Hz).

Vertical pressure amplitude distributions calculated for the first four modes using the zero gradient profile (Fig. 2b) suggest that the modal pressures are approximately symmetrically (odd-numbered modes) or antisymmetrically (even-numbered modes) distributed about the center of the water column. The distributions associated with the negative and positive gradients (Figs. 2a and 2c, respectively) illustrate that the first mode (and only the first mode) has a majority of its energy confined to propagate in the slower sound speed water layer. A mode is considered "confined" to a slower sound speed water layer when its calculated pressure amplitude function has an inflection point at a depth where that function has a nonzero value. Such a mode's wave number k_n will be greater than or equal to the minimum value of the total wave number K possible in the water column (i.e., $K = \omega/\text{maximum value of } c_1(\xi)$). In general, constriction of the modal pressure amplitude distribution requires sharper gradients to confine more and higher order modes.

Table 1
Measured Sound Speeds (in m/sec) for March 1970 Experiment

Depth m	Velocimeter Cast									
	a	b	c	d	e	f	g	h	i	j
0	1513.9	1512.9	1508.7	1508.5	1509.4	1507.0	1508.3	1507.0	1506.2	1505.8
2	1513.9	1512.9	1508.7	1508.5	1509.4	1507.0	1508.3	1507.0	1506.2	1505.8
4	1513.9	1512.9	1508.8	1508.5	1509.4	1507.0	1508.4	1507.1	1506.4	1505.8
6	1513.9	1512.9	1508.8	1508.6	1509.5	1507.3	1508.5	1507.2	1506.4	1505.9
8	1514.0	1513.0	1508.8	1508.6	1509.6	1507.3	1508.4	1507.2	1506.7	1505.9
10	1514.1	1513.1	1508.8	1508.7	1510.1	1508.1	1508.9	1507.5	1506.9	1506.1
12	1514.0	1513.1	1508.9	1508.8	1510.4	1508.6	1510.1	1507.7	1508.8	1511.6
14	1513.8	1513.3	1508.9	1508.8	1511.1	1509.0	1511.5	1508.7	1511.9	1512.2
16	1513.9	1513.6	1508.9	1508.7	1513.3	1510.2	1512.9	1511.0	1512.3	1512.2
18	1512.0	1513.4	1509.0	1508.8	1513.5	1510.2	1513.1	1512.8	1512.4	1512.3
20	1511.3	1511.1	1509.0	1508.9	1513.6	1510.6	1513.1	1512.9	1512.4	1512.3
22	1511.0	1510.1	1509.3	1509.0	1513.6	1511.2	1513.1	1512.9	1512.5	1512.4
24	1510.9	1509.9	1509.3	1509.6	1513.6	1511.2	1513.0	1512.9	1512.5	1512.4
26	1510.9	1509.9	1509.5	1509.5	1513.6	1511.3	1513.0	1513.0	1512.5	1512.4
28	1510.9	1509.9	1509.8	1509.7	1513.7	1511.3	1513.2	1513.1	1512.6	1512.5
30	1510.9	1510.0	1510.0	1510.4	1513.7	1511.4	1513.2	1513.1	1512.6	1512.5
bottom*	1510.9	1510.0	1510.0	1510.4	1513.7	1511.4	1513.2	1513.1	1512.6	1512.5

*The sound speed at the bottom of the water column was estimated by extrapolation of measured values.

Table 2
Environmental Data Associated with
Sound Speed Measurements in Table 1

Veloci- meter Cast	March 1970 Date-Time Group	Range* (km)	Wind Speed (knots)	Wind Direction (T)	Wave Height (m)
a	130000Z	11.9	23	270	1.5
b	121438Z	7.9	†	†	†
c	161659Z	9.9	10	075	1.0
d	161427Z	9.9	20	075	1.0
e	131730Z	7.9	†	†	†
f	170003Z	19.8	12	160	0.5
g	131952Z	9.8	26	295	1.5
h	132354Z	13.7	20	320	1.5
i	160354Z	9.9	18	350	†
j	160033Z	13.9	18	280	1.0

*Range along a 285° T bearing line from Stage I ($30^{\circ}00'06''$ N,
 $85^{\circ}54'03''$ W).

†Data not taken.

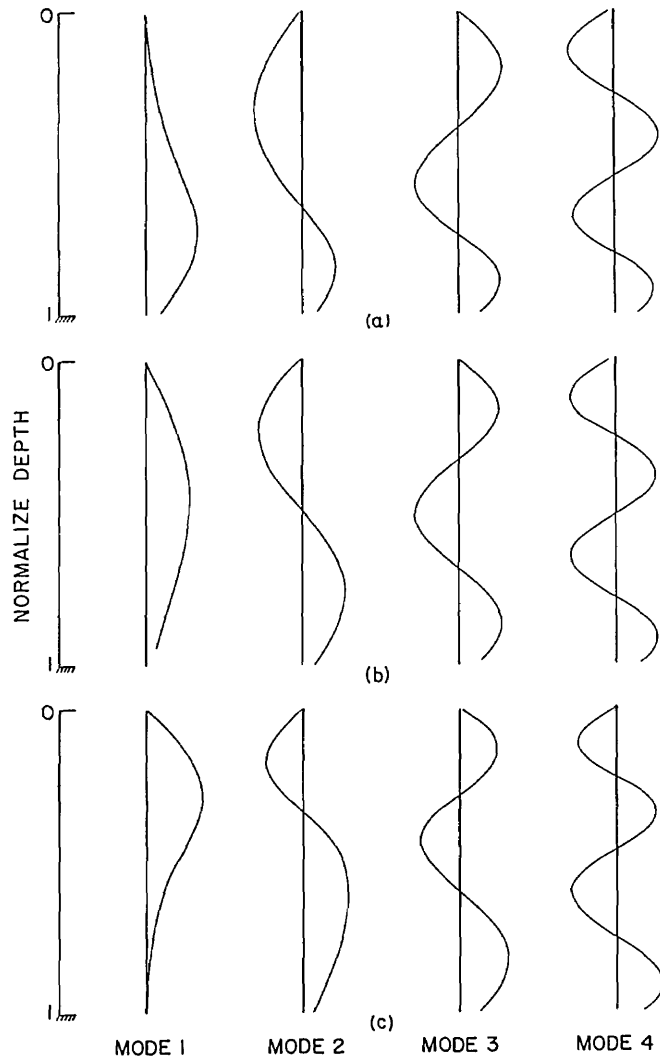


Fig. 2 — Vertical distributions of pressure amplitude of the first four modes at 750 Hz were calculated using three different sound speed profiles from Table 1: (a) negative gradient profile a, (b) isovelocity profile c, and (c) positive gradient profile j.

Group velocity calculations (Fig. 3b) using the zero gradient profile indicate that, for the frequencies shown, mode group velocities decrease with increasing mode number. Sufficiently sharp gradients may change this order (see Figs. 3a and 3c) by confining a majority of the energy of otherwise faster low-order modes to a slower sound speed layer.

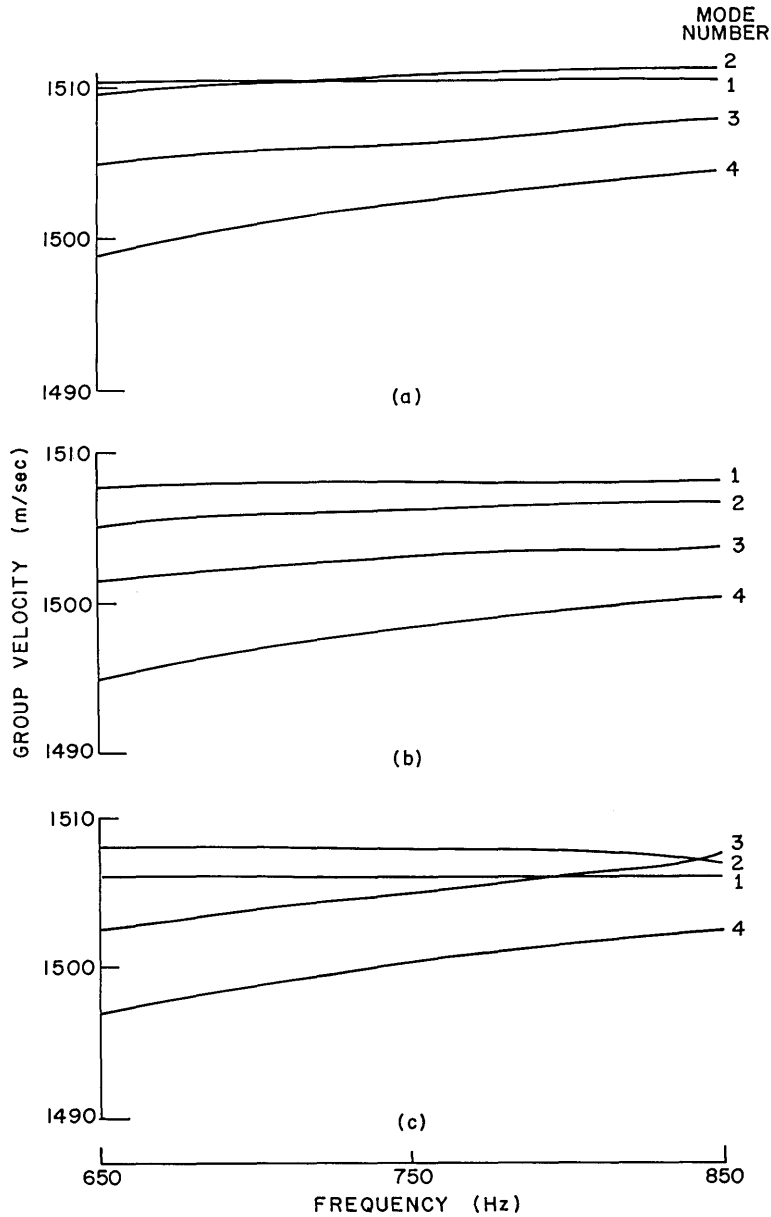


Fig. 3 — Group velocities of the first four modes were calculated using three different sound speed profiles from Table 1: (a) negative gradient profile a, (b) isovelocity profile c, and (c) positive gradient profile j.

Since, for a given bottom and fixed mode number, the mode's pressure amplitude at the bottom increases as the percentage of the mode's total energy that propagates in the bottom increases, it seems reasonable to assume that the bottom attenuation of a mode (that portion of its total attenuation due to interaction with the bottom) would increase as the mode's pressure amplitude at the bottom increases. For a zero- or positive-gradient profile the calculated modal bottom pressure amplitude increases with increasing mode number (Figs. 2b and 2c). However, for negative gradient profiles (Fig. 2a) sufficiently sharp to confine some, but not all, of the modes near the bottom, some higher order unconfined modes may have lower bottom pressure amplitudes than lower order confined modes. The bottom pressure amplitude of the first mode is highest for a confining negative-gradient profile (Fig. 2a), intermediate for an unconfined zero-gradient profile (Fig. 2b), and lowest for a confining positive-gradient profile (Fig. 2c). Such trends have been observed for higher modes when sufficiently strong profiles to confine them were used. Qualitative evidence that the measured total mode attenuation follows the expected attenuation trends for the first and second modes associated with profiles a, c, and j will be presented in the Mode Attenuation Coefficients section.

EXPERIMENTAL PROCEDURES

This section describes details of the March 1970 experiment. Similar information pertaining to the July 1969 experiment is found in Ref. 2. The bottom profile along a 285° true bearing line from Stage I ($30^\circ 00' 06''$ N, $85^\circ 54' 03''$ W) was measured with a shallow-water fathometer over ranges from 0.9 to 17.8 km from the Stage. (Figure 4 depicts the geography.) Readings indicated an average depth of 31.3 m with maximum bottom contour variations of ± 2.5 m. Tidal depth changes measured at Stage I were approximately 0.7 m. The source was rigidly mounted on a carriage that could be lowered and raised on rails attached to Stage I. A vertical line of 12 hydrophones spaced at 2-m increments was lowered over the side of a ship to depths from either 5 to 27 or 6 to 28 m. Each hydrophone was equipped with a preamplifier having 16.3-dB gain. The mechanical Q of the 750-Hz omnidirectional transducer was approximately 4, so acoustic signals did not build up to a maximum possible output level with the three-cycle electrical input pulse. The maximum buildup of the source output corresponded to a source level of 103.2 dB relative to 1 dyne/cm² at 1 m.

Individual runs lasted about 7 min and consisted of approximately 60 three-cycle pulses. Data were recorded and stored by an FM analog tape recorder and subsequently rerecorded by an oscillographic recorder for processing. A block diagram of the recording instrumentation is shown in Fig. 5.

Sound speed profiles were recorded two or three times daily using two adjacently mounted velocimeters. They were lowered to the bottom to dislodge any trapped air bubbles and then raised in 2-m increments to the surface. Table 1 contains all sound speed profiles for 750-Hz runs. Associated environmental data are given in Table 2. A previously conducted acoustic reflectivity experiment (4) yielded estimates of the bottom sound speed and density in the area as 1589 m/s and 1.85 g/cm³, respectively.

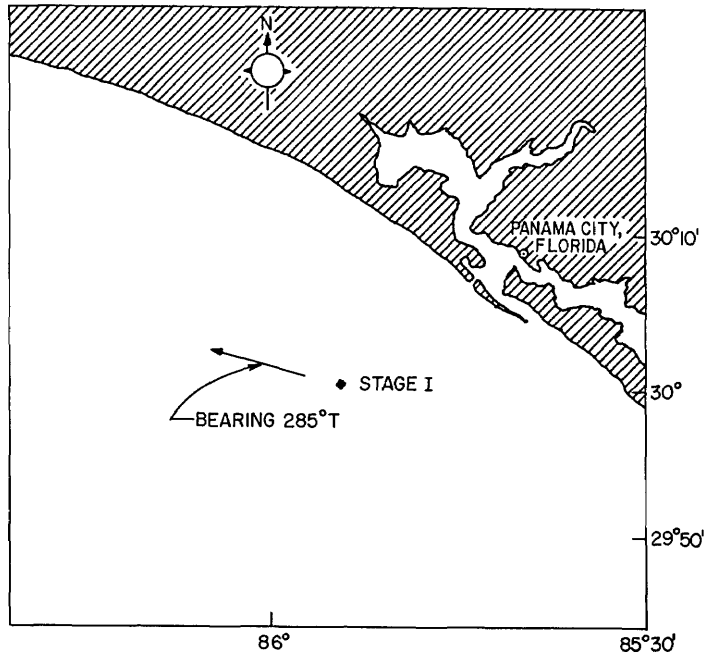


Fig. 4 — Location of July 1969 and March 1970 experiments

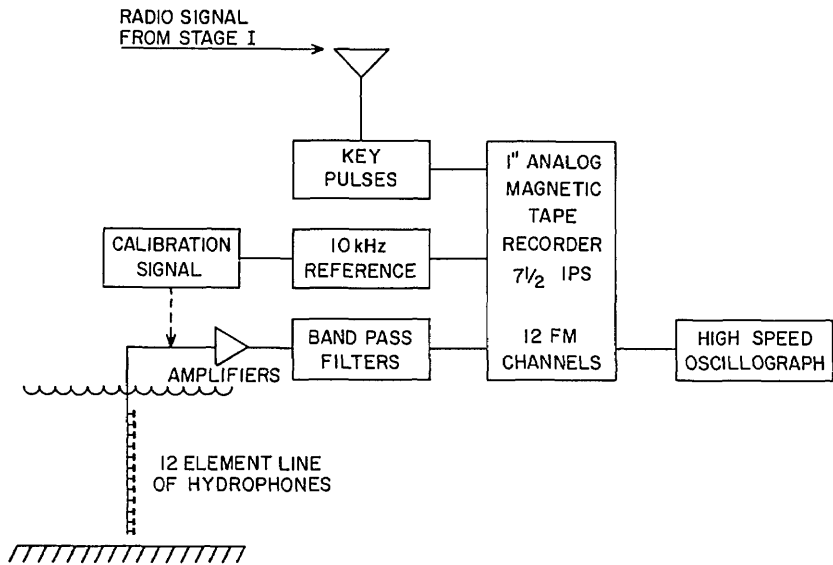


Fig. 5 — Block diagram of recording instrumentation for March 1970 experiment

PROCESSING TECHNIQUES

Mode Resolution by Time of Arrival

If a duct is excited with a pulse of duration T_0 , the components of that pulse propagated in any pair of normal modes of the duct, having group velocities U_m and U_n , will be completely separated in time at range (5)

$$r \geq T_0 U_m U_n / (U_m - U_n). \quad (3)$$

It is assumed here that the pulse is not lengthened significantly by dispersion. Temporal resolution was used to examine individual modal fields whenever group velocities differed sufficiently to produce mode resolution at a range where the available signal-to-noise ratio was adequate. When complete temporal resolution could not be achieved, a spatial processing technique was used to resolve the modes.

Mode Resolution by Spatial Filtering

The set of discrete normal modes established by a source is orthonormal. That is

$$\int_0^1 \rho_1 u_n(\xi) u_m(\xi) d\xi + \int_1^\infty \rho_2 u_n(\xi) u_m(\xi) d\xi = \delta_{mn}, \quad (4)$$

where δ_{mn} is the Kronecker delta.

The orthogonality permits the postulation of an ideal vertical sensing array responding to signals propagating in any one selected mode and rejecting signals propagated in any other mode. In such an array the response and polarities of the individual elements would be adjusted to be proportional to the magnitudes and signs at corresponding depths of the selected mode amplitude function (eigenfunctions). An ideal array would be capable of monitoring a vertical continuum extending from the water's surface down infinitely into the bottom. The sum of the output of all the elements of such an array would be zero for all signals except those propagating in the selected mode as indicated in Eq. (4). In practice such an array can be approximated using a finite number of sensors (in these experiments, 8 or 12) spaced throughout the water column and adjusting their output gains and polarities to match a selected mode either during recording (on line) or processing (playback). The principal limitations on the effectiveness of this array are imposed by three factors.

The first is interchannel phase distortion resulting from anomalies in the magnetic tape recorder (maybe eliminated by on-line processing) and from bowing of the line array by underwater currents. Such distortion degrades the coherent summation of the signals in the 12 input channels resulting in a reduced filter response for the desired mode. Reductions in response of 17% to 22% have been observed.

The second arises from the finite number of discrete samplings of the signal field. Although the modal eigenfunctions, in theory, are orthogonal, the filter may not be completely effective when only a finite sampling of the field is available. Sample calculations for the array used in these experiments indicated that, in most cases, theoretical rejection

of at least 10 dB could be achieved. Rejections ranging from 12 to 20 dB have been observed experimentally when modes were temporally resolved.

The third is induced by temporal changes in the mode amplitude functions. This decreases both the effective rejection of unwanted modes and the signal enhancement of a chosen mode. It is believed, however, that this was not as important a factor as the first two because there were indications that the mode amplitude function remained relatively stable over short time periods (see Temporal Variations section).

Measurement of Vertical Distributions of Pressure Amplitude

When temporal resolution of a mode was achieved, the pressure amplitude of the modal field was measured at the depth of each of the 12 hydrophones. This provided an experimental measure of the distribution of pressure amplitude with depth. It could also provide 12 independent measurements of the mode attenuation coefficient α_n , since all other quantities in Eq. (1) are known or can be calculated. When mode resolution required the use of the spatial filter, the filter output was used to calculate α_n . This could be done since, if one assumes that the field had the calculated distribution with depth, the filter output can be interpreted either in terms of the mean signal level of a mode averaged over depth, or in terms of the modal signal level at any given depth.

Measurement of Mode Attenuation Coefficients

When the mode filter is matched to the n th mode, its output τ_n is given by

$$\tau_n = K \sum_{i=1}^{12} u_n(\xi_i) p_n(\xi_i), \quad (5)$$

where K is a system gain constant and ξ_i is the depth of the i th hydrophone. If it is assumed that the vertical distribution of pressure amplitude for the n th mode has the same form as $u_n(\xi)$, then the $p_n(\xi)$ can be related to $u_n(\xi)$ by a constant of proportionality ψ_n such that

$$p_n(\xi) = \psi_n u_n(\xi). \quad (6)$$

Substituting Eq. (6) into Eq. (5) and solving for ψ_n , we obtain

$$\psi_n = \tau_n \left\{ K \sum_{i=1}^{12} u_n^2(\xi_i) \right\}^{-1} \quad (7)$$

α_n can be written in terms of ψ_n by substituting Eq. (6) into Eq. (1),

$$\alpha_n = \frac{1}{r} \left\{ S + 20 \log \left[\frac{\sqrt{2\pi} u_n(\xi_0) \rho_1}{H k_n^{1/2}} \right] - 10 \log r \right. \\ \left. + 10 \log \frac{T_0}{T_0 + \Delta T_n} - 20 \log \psi_n \right\}. \quad (8)$$

RESULTS

Comparison of Measured and Calculated Vertical Distribution of Pressure Amplitude

A normal mode computer program (3), supplied with the previously stipulated environmental information, calculated theoretical mode amplitude functions (eigenfunctions), phase and group velocities, and mode wavenumbers.

Experimental vertical distributions of pressure amplitude were measured for five runs in which modes were sufficiently well resolved. The theoretical and experimental distributions for these runs, accompanied by the sound speed profiles used to calculate the theoretical mode amplitude functions, are shown in Figs. 6a through 6e. Only the first and second modes had sufficient intensity to be identified and measured. Maximum peak-to-peak deflections for signals propagated in those modes were measured from each of the oscillographic recorder channels for ten pulses uniformly distributed throughout a run. The average of the ten measurements from each channel was plotted at the normalized depth of the hydrophone associated with that channel. (A phase shift of approximately 180° was observed in received signals whenever the pressure amplitude of the second mode crossed a zero value.) The resulting experimental mode amplitude values and polarities (dots) were then displayed with the calculated mode amplitude functions (solid lines) after an amplitude adjustment using a scaling constant that equated their maxima. Three runs were from the March 1970 experiment (750-Hz source frequency, positive gradient, and nearly isovelocity sound speed profiles — Figs. 6a, 6b, and 6c); two runs were taken from the July 1969 experiment (400-Hz source frequency, negative gradient sound speed profiles — Figs. 6d and 6e).

The agreement between calculated and measured mode amplitude functions indicates that, in these cases, a reasonably accurate prediction of mode amplitude distribution with depth was possible. The slight variations in the measured first-mode amplitudes from their calculated values near the bottom of Fig. 6a and near the top of Fig. 6d are believed to be caused by the arrival of the third mode. The group velocity of the third mode at the source center frequencies was nearly, but not exactly, the same as that of the first mode in these two runs.

Mode Attenuation Coefficients

Mode attenuation coefficients α_n were calculated using Eq. (8) and measured τ_n values (see Eq. (7)) for several runs for 400 Hz, first mode, and 750 Hz, first and second modes. Intensities were calculated for each pulse from the adder output and then averaged to obtain a time-averaged value of intensity for a run. Table 3 shows the α_n values determined from the time-averaged intensity and velocimeter cast identifications (these velocimeter cast measurements are found in Ref. 2) for the 400-Hz runs. Since intensity values fluctuated significantly during some of the 750-Hz runs, the α_n values corresponding to the minimum and maximum intensity values of a single pulse for each run are also displayed with the time-averaged α_n values in Table 4. Both tables contain values of $c_1(1) - c_1(0)$ to express differences in the water layer's bottom and surface sound speeds for the prevailing profiles. (Since all profiles were essentially monotonic and differences in sound speed, if any, were generally localized within similar depth intervals, these values are indicative of relative strengths of the sound speed gradients.) The tables include only

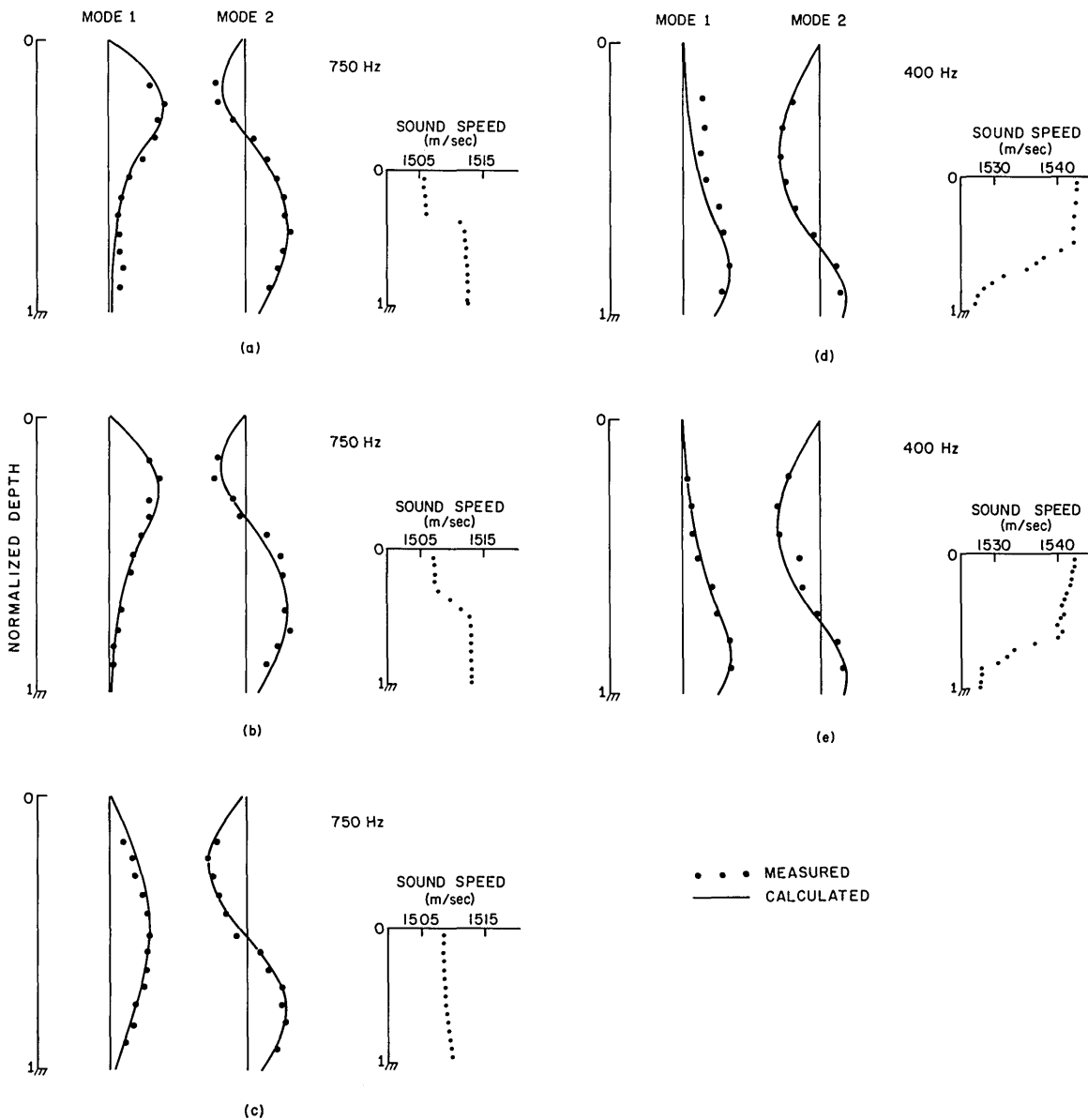


Fig. 6 — Measured and calculated vertical distributions of pressure amplitude are plotted for the first and second modes of five runs in which these modes were completely separated by time of arrival. Also included are plots of the velocimeter cast measurements associated with each run.

Table 3
 Mode Attenuation Coefficients at 400 Hz: Time-Averaged Values for Each of Several Runs. $c_1(1) - c_1(0)$ Represents Difference Between the Water Layer's Bottom and Surface Sound Speeds.

Mode 1

Velocimeter Cast*	$c_1(1) - c_1(0)$ (m/s)	α_1 (dB/km)
11-3	-17.3	1.48
6-1	-16.0	0.89
1-6	-15.8	2.36
2-1	-15.8	1.70
6-5	-15.7	2.02
11-5	-15.0	1.36
12-2	-14.5	1.57
9-6	-13.6	1.72

*Velocimeter casts found in Ref. 2.

Table 4
 Mode Attenuation Coefficients at 750 Hz: Minimum, Maximum, and Time-Averaged Values for Each of Several Runs. $c_1(1) - c_1(0)$ Represents Difference Between the Water Layer's Bottom and Surface Sound Speeds.

Mode 1

Velocimeter Cast	$c_1(1) - c_1(0)$ (m/s)	α_1 min (dB/km)	α_1 max (dB/km)	$\bar{\alpha}_1$ (dB/km)
a	-3.0	1.29	1.64	1.49
c	1.3	-0.11	0.37	0.13
d	1.9	-0.10	0.25	0.05
e	4.3	0.07	0.53	0.28
f	4.4	0.29	0.52	0.45
g	4.9	0.14	0.57	0.35
h	6.1	0.41	1.00	0.84
i	6.4	-0.30	-0.08	-0.19
j	6.7	0.03	0.18	0.12

Mode 2

Velocimeter Cast	$c_1(1) - c_1(0)$ (m/s)	α_2 min (dB/km)	α_2 max (dB/km)	$\bar{\alpha}_2$ (dB/km)
b	-2.9	0.53	0.87	0.64
c	1.3	0.14	0.72	0.45
d	1.9	0.37	0.96	0.77
g	4.9	0.02	0.91	0.63
g	4.9	0.45	1.25	0.92
h	6.1	0.94	1.41	1.26
j	6.7	0.62	1.04	0.85
j	6.7	0.67	0.90	0.81

those data obtained from runs where the mode eigenfunction value at the source's depth was at least 75% of its maximum value in the water column. The weaker modal signals resulting from less mode excitation (see Eq. (1)) for the remaining runs were judged too small to be confidently distinguished from the background noise.

Table 3 shows generally higher first-mode attenuation values for 400-Hz than for the 750-Hz values shown in Table 4. Although one might, in general, expect a decrease in attenuation for a lowering of frequency (6), it is believed that the increased bottom interaction caused by the very sharp negative gradients associated only with the 400-Hz runs were sufficient to increase their attenuation enough to obscure the effect of a decreased source frequency.

Relations among mode number, sound speed gradients, and the measured attenuation maybe observed in Table 4. Primarily, an increase in attenuation accompanies an increase in mode number for all positive and isovelocity profiles. The negative-gradient (profile a), first-mode run, however, had the highest attenuation in Table 4. The first mode of this run, unlike any of the others in Table 4, had a majority of its energy confined to propagate in the slower water layer near the bottom. These relations parallel those that might be expected if only that portion of modal attenuation due to the mode's interaction with the bottom were considered, and consequently imply a strong dependence of total modal attenuation on modal interaction with the bottom.

For cases in which modes interact relatively weakly with the bottom (for example, see first-mode attenuation in Table 4, velocimeter casts *c* through *j*), other attenuation mechanisms might be expected to predominate. Attenuation for confining positive gradients may vary because of interactions with the surface, such as scattering, and could possibly depend on the sea state.

Temporal Variations

Temporal variations of the modal intensities determined from the mode filter output were observed in the 750-Hz runs from which attenuation coefficients were obtained (see Table 4). Plots of these depth-averaged intensities *vs* time for the first and second modes are shown in Figs. 7a and 7b, respectively. The lower case letter by each run designates the velocimeter cast associated with that run (see Table 1). These temporal variations could be caused by changes in the pressure amplitude distribution or by fluctuations of mode attenuation or excitation. A test was conducted in an attempt to clarify the source of the temporal variations.

In this test, temporal fluctuations of the amplitude of modal arrivals at individual hydrophones were compared with the temporal fluctuations of the filter output. The maximum amplitude of each signal propagated in a particular mode was measured for a sequence of approximately 60 pulses, both at the output of an individual hydrophone and at the output of the mode filter matched to that mode. A cross-correlation coefficient was then calculated for those sequences using

$$R_n = \left[\sum_{i=1}^I (x_i - \bar{x}) (u_i - \bar{y}) \right] \left[\sum_{j=1}^I (x_0 - \bar{x})^2 \sum_{i=1}^I (y_i - \bar{y})^2 \right]^{-1/2}, \quad (9)$$

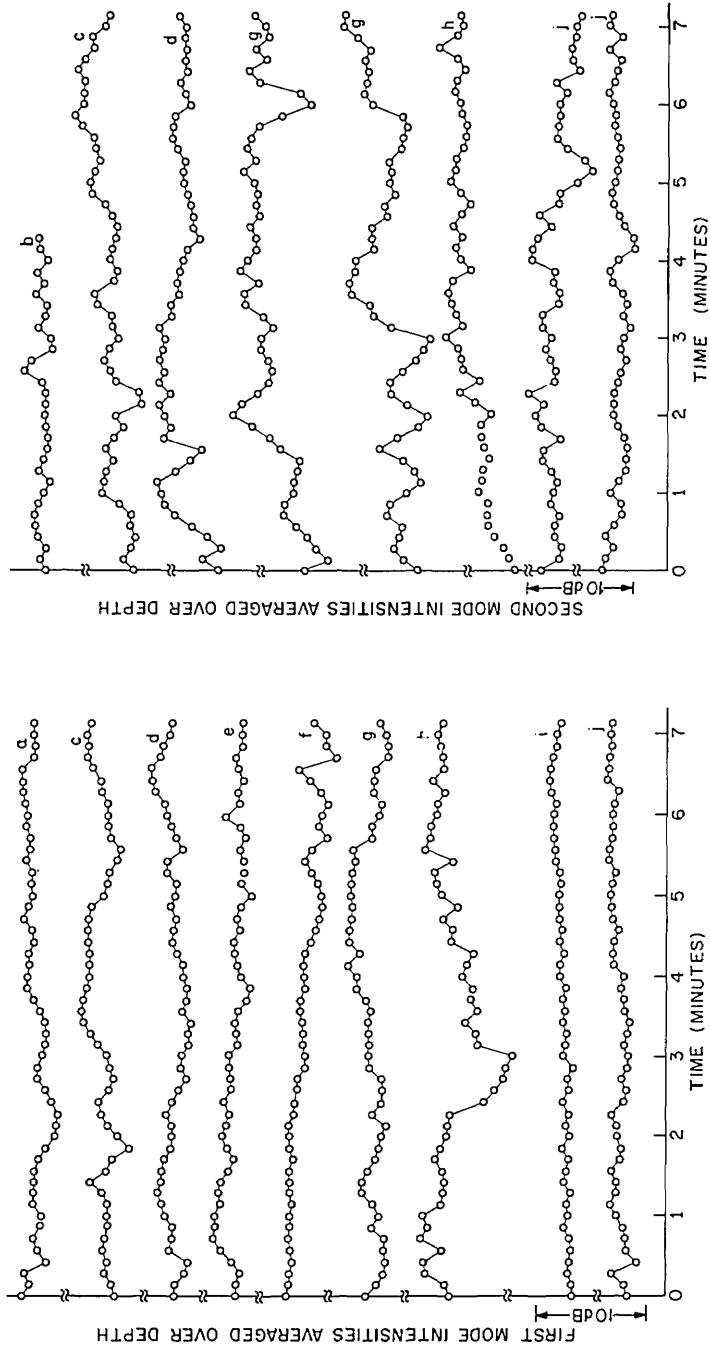


Fig. 7a — The time histories of first-mode intensities averaged over depth are plotted for nine different runs. The letter following each run identifies the associated velocimeter cast (see Table 1).

Fig. 7b — The time histories of second-mode intensities averaged over depth are plotted for eight different runs. The letter following each run identifies the associated velocimeter cast (see Table 1).

where

- R_n = n th mode's cross-correlation coefficient
 I = total number of pulses in a run
 x_i and y_i = outputs of an individual hydrophone and the mode filter, respectively,
 for the i th pulse
 \bar{x} and \bar{y} = arithmetic means of those outputs over I pulses.

When this was done for several hydrophones in each of two runs the correlation coefficients for the first mode ranged from 0.72 to 0.92. For the second mode they ranged from 0.56 to 0.92. The correlations obtained tend to indicate that at least the major features of the temporal fluctuations observed at discrete depths coincided with those of the field averaged over depth. Thus, it appears that the major cause of the observed fluctuations is associated with changes in total field strength rather than with changing distributions. Further evidence of this can be observed in Figs. 6a through 6e where the time-averaged measured distributions agree well with the calculated distribution.

On the other hand, the very large (up to 9 dB at 10 km in 7 min) changes in signal level shown in Figs. 7a and 7b are difficult to account for through variable attenuation mechanisms. However, one might expect the vertical pressure amplitude distribution of the measured modes to be more strongly dependent on environmental conditions in the vicinity of the receiving hydrophones. If this were the case, environmental conditions more distant from those hydrophones might affect the average modal signal amplitudes without significantly altering the distributions.

CONCLUSIONS

Comparisons of measured and calculated vertical distributions of pressure amplitude for the first two modes of 400- and 750-Hz signals demonstrated that such distributions could be measured and predicted in at least one simple experimental geometry for various sound speed profiles including positive, zero, and negative gradients. It remains to extend these capabilities to areas of different bottom types and more complicated bottom contours.

The prediction of the pressure amplitude distribution with depth proved sufficiently accurate to encourage the development of a spatial mode filtering technique based on the inherent orthogonality of normal modes. Such a filtering technique was used to determine individual mode intensities averaged over depth.

Mode intensity variations of up to 9 dB at a range of 10 km were observed within 7-min runs. Specific causes of these variations are not known. Various cross-correlation tests tended to indicate, however, that the vertical distributions of pressure amplitude remained relatively stable. Therefore, fluctuations in attenuation mechanisms that affect the total signal field uniformly with depth at the receiving line of hydrophones are suspected to be the predominant sources of the observed mode intensity variations.

The average attenuation values of the first two modes for several runs were determined from the mode intensity measurements. Relations among mode numbers, sound speed gradients, and attenuation values showed an observable dependence of the modal attenuation on the degree to which the mode interacts with the bottom. (Attenuation increasing with increasing bottom interaction.) For situations where positive gradients are sufficiently sharp to confine modes to water layers near the top, attenuation mechanisms other than those associated with the bottom may become prevalent.

ACKNOWLEDGMENTS

The author expresses his gratitude to Raymond H. Ferris for his guidance; Frank Ingenito, Stephen N. Wolf, and John DeSanto for their advice; Alfred V. Newman for his assistance; and Joanne F. Peery for her patience.

REFERENCES

1. I. Tolstoy and C.S. Clay, *Ocean Acoustics: Theory and Experiment in Underwater Sound*, McGraw-Hill, New York, 1966, Chap. 3, 4
2. R.H. Ferris, F. Ingenito, and A.L. Faber, "Experimental Separation and Identification of Acoustic Normal Modes in Shallow Water," NRL Report 7174, Oct. 30, 1970
3. A.V. Newman and F. Ingenito, "A Normal Mode Computer Program for Calculating Sound Propagation in Shallow Water with an Arbitrary Velocity Profile," NRL Memo Report 2381, Jan. 1972
4. R.H. Ferris and W.A. Kuperman, "An Experiment on Acoustic Reflection from the Sea Surface," NRL Report 7075, May 28, 1970
5. R.H. Ferris, "A Comparison of Measured and Calculated Normal Mode Amplitude Functions for Acoustic Waves in Shallow Water," *J. Acoust. Soc. Amer.* 52 981-988 (Sept. 1972)
6. R.S. Anderson and A. Blackman, "Attenuation of Low-Frequency Sound Waves in Sediments," *J. Acoust. Soc. Amer.* 49, 786-791 (Mar. 1971)

DOCUMENT CONTROL DATA - R & D

(Security classification of title, body of abstract and indexing annotation must be entered when the overall report is classified)

1. ORIGINATING ACTIVITY (Corporate author) Naval Research Laboratory Washington, D.C. 20390		2a. REPORT SECURITY CLASSIFICATION Unclassified	
		2b. GROUP	
3. REPORT TITLE SOME MEASUREMENTS OF ACOUSTIC NORMAL MODE PROPAGATION IN SHALLOW WATER			
4. DESCRIPTIVE NOTES (Type of report and inclusive dates) Interim report; work is continuing on the problem.			
5. AUTHOR(S) (First name, middle initial, last name) A.F. Schuetz			
6. REPORT DATE November 16, 1972	7a. TOTAL NO. OF PAGES 22	7b. NO. OF REFS 6	
8a. CONTRACT OR GRANT NO. NRL Problem S01-45	9a. ORIGINATOR'S REPORT NUMBER(S) NRL Report 7493		
b. PROJECT NO. RF 05-552-404-5350	9b. OTHER REPORT NO(S) (Any other numbers that may be assigned this report)		
c. SF 52552-070			
10. DISTRIBUTION STATEMENT Approved for public release; distribution unlimited.			
11. SUPPLEMENTARY NOTES		12. SPONSORING MILITARY ACTIVITY Department of the Navy (Office of Naval Research, Arlington, Va. 22217), and Naval Ship Systems Command, Washington, D.C. 20360.	
13. ABSTRACT Experiments were conducted in the northern Gulf of Mexico (30°00'06"N, 85°54'03"W) during July 1969 and March 1970 to study propagation characteristics of acoustic normal modes. This shallow-water area had a constant depth (31 ± 2.5 m) over a propagation path of at least 20 km along a bearing line of 285°T. Short-pulse, 3 cycle signals were emitted from 400- or 750-Hz center frequency sources. The vertical distributions of pressure amplitude of each of the two lowest order normal modes of these signals, measured by a vertical line of hydrophones, agreed well with distributions calculated by computer using a two-layer fluid model. Temporal variations of modal intensity averaged over depth for both the first and the second modes were observed for 7-min runs. Although the specific causes of these variations were not determined, there were indications that the vertical distributions of pressure amplitude remained comparatively stable and signal fluctuations were occurring uniformly with depth. Time-averaged attenuation coefficients were also obtained for the first and second modes for 7-min runs. When a mode was predicted to interact strongly with the bottom, its measured attenuation was high compared to cases where that mode was predicted to interact weakly with the bottom.			

14. KEY WORDS	LINK A		LINK B		LINK C	
	ROLE	WT	ROLE	WT	ROLE	WT
Underwater acoustics						
Shallow water						
Normal modes						
Experimental results						
Vertical pressure amplitude distributions						
Attenuation						
Temporal stability						